DOI: 10.1002/ejic.200700953

Yttrium, Lanthanide and Mixed Y-Ln Vanadates Prepared from Molecular Precursors Based on EDTA

Nicolas Deligne,[a] Vanessa Gonze,[a] Daisy Bayot,[a] and Michel Devillers*[a]

Keywords: Vanadates / Lanthanides / EDTA / Molecular precursors / Mixed oxides

Yttrium(III) and lanthanide(III) vanadates corresponding to the general formula AVO_4 (A = Y, Pr, Sm, Eu, Gd, Dy, Er) were prepared by a nonconventional soft chemistry route in which coordination compounds of the different elements to be incorporated were used as molecular precursors. In this case, EDTA-based yttrium(III), lanthanide(III) and vanadium(V) complexes were synthesised, characterised and used as precursors for the preparation of zircon-type AVO_4 materials at a moderate temperature of 800 °C, as evidenced by XRD and Raman analyses. Solid solutions such as $Y_{1-x}Pr_xVO_4$ and $Y_{1-x}Gd_xVO_4$ were also obtained. Linear correlations between chemical compositions and lattice parameters or Raman shifts were observed. SEM was used to characterise the particle size and morphology.

Introduction

Yttrium vanadate (YVO_4) and lanthanide vanadates ($LnVO_4$) generate considerable interest due to their interesting electric, optical, magnetic and catalytic properties. Among others, it was recently shown that rare earth orthovanadates can be very attractive for oxidative dehydrogenation of light alkanes and, in this context, $SmVO_4$ seems to be one of the most promising systems.[1] Furthermore, materials based on $CeVO_4$ could be involved in various potential applications such as counter electrodes in electrochromic devices, gas sensors, and components of oxide fuel cell anodes.[2] $LnVO_4$ compounds have also been extensively studied for their magnetic properties and cooperative Jahn–Teller distortions.[3] For instance, it was shown that $DyVO_4$ undergoes a crystallographic distortion from tetragonal to orthorhombic at 14 K and a magnetic transition to an antiferromagnetic state at 3 K.[4] Besides this, yttrium and lanthanide orthovanadates are mostly known as adequate hosts for rare earth activators. Eu^{3+}-doped YVO_4 was first proposed by Levine and Palilla[5] as a phosphor for colour television tubes and subsequently used for a long time in those devices.[6] When activated with Nd^{3+}, $GdVO_4$ crystals are very interesting materials for diode-pumped microlaser systems.[7]

Such multimetallic oxides are classically prepared by standard procedures such as the conventional solid-state method. This method was successfully implemented for lanthanide vanadates but generally requires high temperatures (>1000 °C), long reaction times and intermediate grindings.[8] These conditions lead usually to irregular and quite large particles due to the increase of the sintering effect with temperature. The particular interest for such vanadates as inorganic phosphors and the combined influence of purity and morphology of the oxides on their optical properties has recently led to an extensive research in the development of alternative synthesis methods. This is particularly true for the famous Eu^{3+}-activated YVO_4. In this context, the most common routes are colloidal methods,[9] hydrothermal routes,[10] the citrate method[11] and co-precipitation.[12] Recently, a modified polyacrylamide gel method was successfully implemented to prepare YVO_4:Eu by addition of a chelating agent, namely citric acid.[13] Besides this, an in situ chemical co-precipitation method was employed by Yan et al. to prepare YVO_4-based microcrystalline phosphors.[14] All these methods allow the preparation of pure zircon-type AVO_4 materials, and sometimes a good control of the particle morphology is possible. Unfortunately, in these routes, the oxide precursors are usually not well defined at the molecular level. For instance, in the case of the citrate method, the precursor is a three-dimensional network where the metal ions are coordinated by one or several citrate molecules.

Since several years, our group aims at developing an alternative approach to multimetallic oxides. The method consists of using, for the different elements to be incorporated, molecular precursors that are stoichiometrically well-defined coordination compounds. The multimetallic oxide materials are obtained by an appropriate thermal treatment in air of a solid homogeneous mixture of the various complexes. This molecular route was shown to allow the preparation of several pure oxide materials under soft conditions, namely lower temperatures and shorter calcination times

[a] Unité de Chimie des Matériaux Inorganiques et Organiques, Université Catholique de Louvain,
Place Louis Pasteur 1, 1348 Louvain-la-Neuve, Belgium
Fax: +32-10-472330
E-mail: devillers@chim.ucl.ac.be

than most other routes. Furthermore, in some cases, a control of the particle morphology was possible. Among others, this approach was successfully implemented for Bi-La and Bi-Pr oxides[15] as well as Nb-Mo, Nb-Ta and Nb-Ta-Bi oxides.[16,17] To the best of our knowledge, in the field of V^V-based materials, only Nb-Ta-V oxides were synthesised according to this soft chemistry route.[16]

This work aims at developing this alternative approach to prepare vanadate hosts, and focuses on the consequences of the preparation method on the properties. For that purpose, EDTA-based complexes of the general formula $(NH_4)[A^{III}(EDTA)]\cdot xH_2O$ and $(NH_4)_3[V^V(O)_2(EDTA)]\cdot 0.5H_2O$ were synthesised, characterised and used as precursors for the preparation of zircon-type AVO_4 host compounds (A = Y or Ln).

Results and Discussion

General Comments on the Oxides Synthesis

The AVO_4 materials were prepared according to the molecular precursor method by using EDTA complexes of the general formula $(NH_4)[A^{III}(EDTA)]\cdot xH_2O$ (A = Y, Pr, Sm, Eu, Gd, Dy, Er) and $(NH_4)_3[V^V(O)_2(EDTA)]\cdot 0.5H_2O$. The A complexes were synthesised from simple oxides or carbonates in basic medium according to an adapted pathway previously described in the literature for mononuclear La^{III} and Pr^{III} complexes.[18] The synthetic pathways and crystallographic structures of all these complexes are already described in the literature, either with ammonium or an alkaline cation.[19] The vanadium precursor was obtained from NH_4VO_3 and H_4EDTA in basic medium according to a described procedure.[16] The A-V-O mixed oxides were then prepared by mixing aqueous solutions of the corresponding complexes and, after removal of the solvent under reduced pressure, the solid mixed precursor was calcined in air to form the final oxide.

Thermal Behaviour of the Precursors

The thermal decomposition of the synthesised complexes and mixed precursors was monitored by thermogravimetric analysis. Figure 1 illustrates the TG curves obtained for two particular complexes, namely $(NH_4)[Y^{III}(EDTA)]\cdot 3H_2O$ (straight line) and $(NH_4)_3[V^V(O)_2(EDTA)]\cdot 0.5H_2O$ (dotted line) and for the corresponding mixed precursor (dashed line), containing the same complexes in stoichiometric amounts. In all cases, the first weight losses are attributed to dehydration. This step extends sometimes up to a surprisingly high temperature of 250 °C, which is attributed to the release of crystallisation and/or coordination water molecules. Unfortunately, the nature of the weight loss at these temperatures is sometimes ambiguous. The position of the last dehydration step is therefore confirmed by the match between theoretical and experimental residual weight values and by elemental analyses. Thanks to these analytical methods, a formula can indeed be proposed for the prepared complexes including the number of water molecules. After the loss of these water molecules, the degradation of the precursor follows with a multistep scheme to produce the simple or mixed oxide.

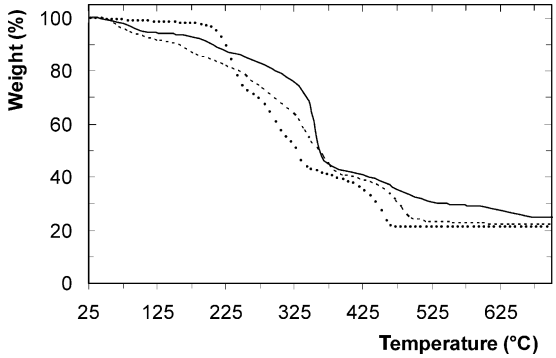

Figure 1. Thermogravimetric analysis under air of $(NH_4)[Y^{III}(EDTA)]\cdot 3H_2O$ (straight line), $(NH_4)_3[V^V(O)_2(EDTA)]\cdot 0.5H_2O$ (dotted line), and (b) the Y-V-O mixed precursor (dashed line).

The DTA curves provide additional information about the nature of the weight losses: the release of water is an endothermic process, whereas the decomposition of the organic matrix is exothermic. Figure 2 displays the TGA and DTA curves obtained for $(NH_4)[Y^{III}(EDTA)]\cdot 3H_2O$. In this case, the weight losses at about 100 and 200 °C can be assigned to dehydration and the highly exothermic steps at 350 and 450 °C to the decomposition of the coordination compound itself. The final decomposition temperature lies between 500 °C for the vanadium complex and 700 °C for the A complexes (A = Y or Ln). It is also interesting to notice that the TG curve of the Y-V-O mixed precursor does not correspond to a superposition of the TG curves of the concerned mononuclear complexes and that its final decomposition temperature is quite lower than that of the most stable simple complex, namely $(NH_4)[Y^{III}(EDTA)]\cdot 3H_2O$ (see Figure 1). This result suggests a homogeneous distribution at the molecular level of the two complexes in the mixed precursor, which is ensured by the preparation pathway, and facilitates the ongoing reaction that produces the vanadate compound.

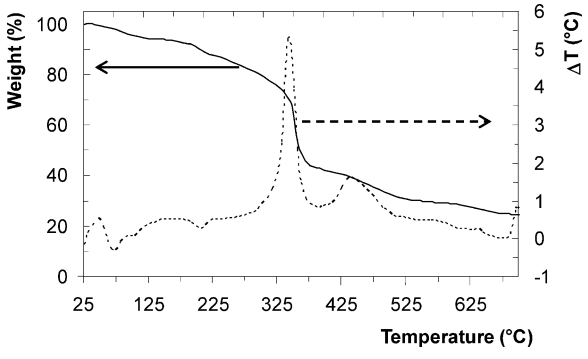

Figure 2. Thermogravimetric analysis (straight line) and differential thermal analysis (dashed line) under air of $(NH_4)[Y^{III}(EDTA)]\cdot 3H_2O$.

AVO_4 Compounds

In order to determine the ideal conditions to prepare pure AVO_4 oxides, X-ray thermodiffractometry was carried out on a selected number of mixed precursors. For that purpose, X-ray diffraction patterns were recorded at various temperatures and again at room temperature at the end. Figure 3 illustrates the results obtained for the Y-V-O precursor.

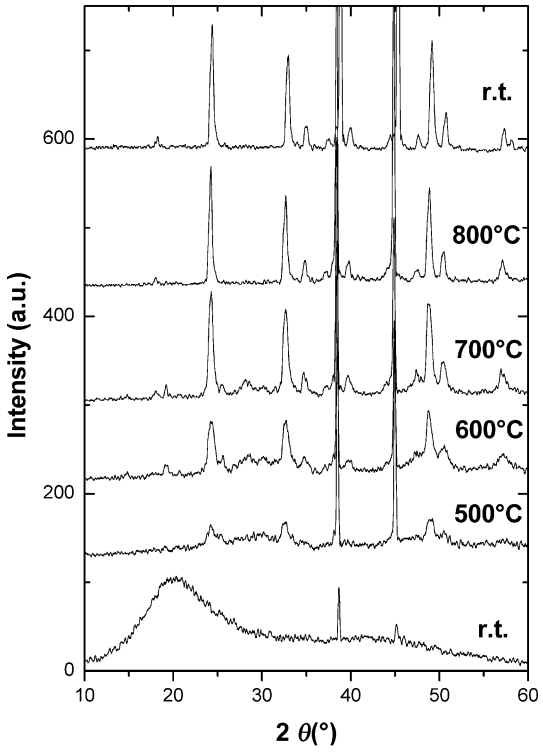

Figure 3. X-ray thermodiffractograms of the Y-V-O mixed precursor obtained after precalcination at 300 °C for 2 h. Patterns are recorded at room temp., between 500 and 800 °C and then again at room temp. (from bottom to top).

According to these results, the oxide phase begins already to crystallise at a temperature of 500 °C and the crystallinity of the material increases when the temperature rises. Almost all the lines observed in the XRD patterns correspond to the zircon-type phase, YVO_4 (JCPDS file 17-0341) except the lines at $2\theta \approx 39$ and 45°, which occur from the platinum support. From 500 to 700 °C, small amounts of simple oxides Y_2O_3 ($2\theta \approx 29°$) and V_2O_5 ($2\theta \approx 20$, 26 and 32°) are also observed but the corresponding peaks disappear when the temperature reaches 800 °C. A temperature of 800 °C seems therefore sufficient to generate the oxide in a pure form and with a good crystallinity. Finally, no structural modification appears when the sample is cooled down and the zircon-type phase is stabilised at room temperature. A thermal treatment of the precursor at higher temperatures, namely 900 and 1000 °C, was also performed and does not improve the crystallinity of the materials. A $Y_{0.5}Pr_{0.5}VO_4$ precursor was also analysed by X-ray thermodiffractometry. In this case, the oxide phase appears to crystallise at a temperature of 600 °C, and the highest crystallinity of the oxide is obtained at a temperature of 800 °C. The formation of pure AVO_4 compounds under such soft conditions, compared with other conventional routes, is probably due to the homogeneous distribution of the various metallic precursors in solution and at the solid state, improving thereby the reaction efficiency.

According to these results, various AVO_4 materials were prepared under air at a temperature of 800 °C, and the purity of the oxide phases was checked by XRD and Raman spectroscopy. As already described in the literature for more conventional methods, yttrium and lanthanide vanadates crystallise in the tetragonal zircon structure ($ZrSiO_4$-type) whatever the nature of the metal ion. It was found that this phase transforms into the denser scheelite structure ($CaWO_4$-type) at a pressure of a few kbar and a temperature less than 600 °C.[12,20] Figure 4 illustrates typical examples of the XRD pattern obtained for the prepared AVO_4 materials. It appears that the various AVO_4 compounds exhibit the same XRD pattern and are consequently isomorphous materials. The observed diffraction lines are all attributed to the zircon-type phase.

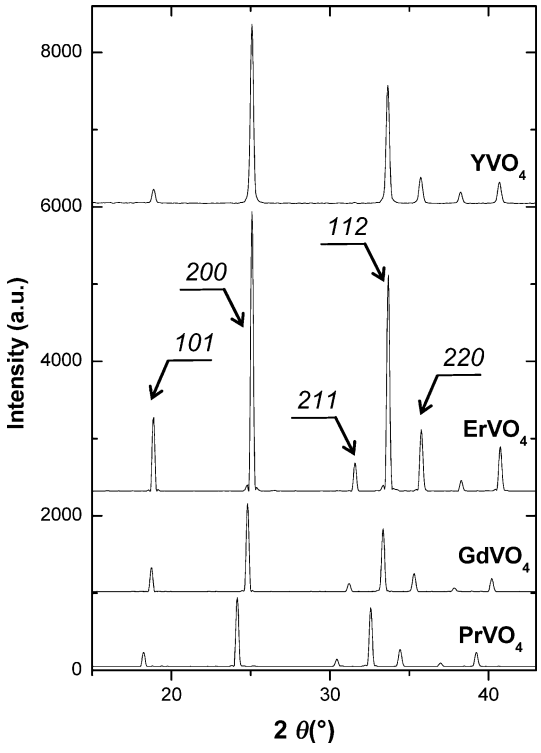

Figure 4. X-ray diffraction patterns of AVO_4 materials with A = Pr, Gd, Er and Y obtained after precalcination of the molecular precursor at 300 °C for 2 h and at 800 °C for 6 h.

However, a slight shift of these lines is observed as a function of the metal ion. This can be easily rationalised by the differences between ionic radii of yttrium and the

lanthanides for a coordination number of 8.[21] An increase of this radius leads to a lattice expansion and consequently to a decrease of the 2θ values. In this work, lattice parameters were determined by means of the position of two main peaks corresponding to the (200) and (112) Miller indices and are listed in Table 1. Figure 5 illustrates the evolution of the lattice parameters as a function of the ionic radius. These results suggest a linear increase of *a*, *b* and *c* lattice parameters when the ionic radius increases. It is also interesting to notice that the lattice expansion is not isotropic and that the increase is slightly higher for *a* and *b* than for *c*. Indeed, *a* and *b* run from 7.10 to 7.37 Å (Er to Pr) whereas *c* parameter runs from 6.28 to 6.47 Å.

Table 1. The A ionic radius and lattice parameters *a* and *c* for the various AVO_4 compounds prepared by the molecular precursor method.

AVO_4	A ionic radius[21] [pm]	*a* [Å]	*c* [Å]
$ErVO_4$	114.4	7.10	6.28
YVO_4	115.9	7.10	6.28
$DyVO_4$	116.7	7.12	6.29
$GdVO_4$	119.3	7.18	6.33
$EuVO_4$	120.6	7.21	6.36
$SmVO_4$	121.9	7.26	6.39
$PrVO_4$	126.6	7.37	6.47

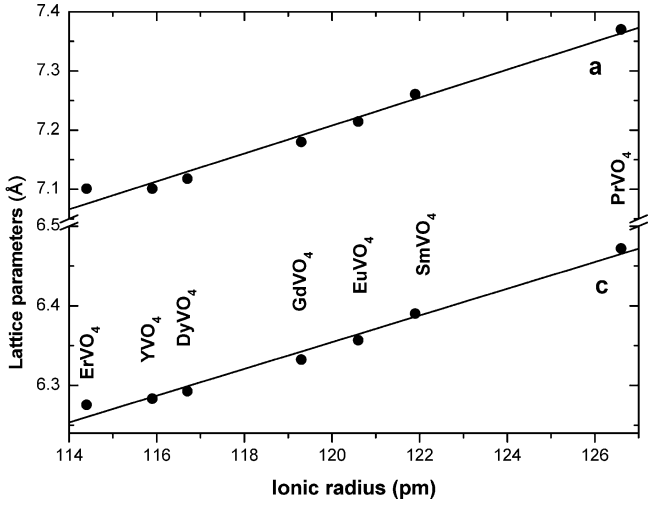

Figure 5. Evolution of the lattice parameter *a* (= *b*) and *c* as a function of the A ionic radius in AVO_4 compounds prepared by the molecular precursor method.

Raman spectra of the prepared AVO_4 materials were also recorded in order to confirm the XRD results. All the samples prepared exhibit similar Raman spectra (Figure 6), and no characteristic band from the simple oxides is observed. The position of the Raman bands observed is in accordance with the literature[22,23] and the results obtained for YVO_4 and $EuVO_4$ as well as their symmetry designation are presented in Table 2. The various modes are separated into internal (internal motions of the tetrahedral VO_4 group) and external modes (translations and rotations of the VO_4 group with respect to the Y ion). According to the literature,[22] the internal B_g mode and the external E_g mode are degenerated in YVO_4 but can be easily distinguished in $LnVO_4$ (see Figure 6).

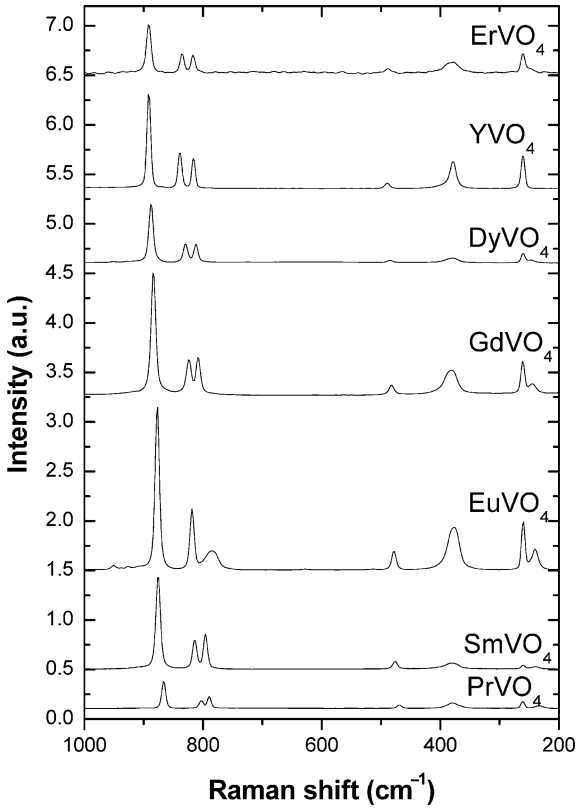

Figure 6. Raman spectra of various AVO_4 materials prepared by the molecular precursor method ($EuVO_4$: *I*/2; $ErVO_4$: *I*×5).

Table 2. Observed Raman shifts [cm^{-1}] and their symmetry designation[22] for YVO_4 and $EuVO_4$ prepared by the molecular precursor method.

Symmetry designation[22]	Raman shift [cm^{-1}]	
	YVO_4	$EuVO_4$
External mode (translation)		
E_g	261	240
Internal modes		
B_g	261	260
A_g	378	375
B_g	489	478
B_g	816	781
E_g	839	818
A_g	891	888

A slight but significant shift of the Raman bands is observed when the A ion is changed. In particular, the band at ca. 880 cm^{-1}, assigned to the V–O vibration,[22] shifts according to the A ionic radius as shown in Figure 7. These results indicate a linear decrease of the Raman shift when

the ionic radius increases. In that context, Escobar and Baran have calculated the force constants for the V–O bond in rare earth vanadates and have shown an increase of the V–O bond strength, from $LaVO_4$ to $LuVO_4$.[24] This increase of the force constant could be responsible for a modification of Raman shifts and it has been attributed to the lattice contraction that can be seen as an increase of the internal pressure. Indeed, it is well known that the Raman shift can be significantly modified by pressure, and this dependence has been previously studied for zircon and scheelite AVO_4 materials.[22,23] The linear evolution of Raman shifts is therefore not surprising as the lattice volume also linearly increases with the lanthanide ionic radius. Furthermore, the decrease of the atomic weight from Er to Pr could also be partially responsible for the decrease of the Raman shift. It is therefore surprising that Raman shifts in YVO_4 have approximately the same value as in $ErVO_4$ although the atomic weight of Y is about twice lower than that of Er. This result seems to show that the A atomic weight has very little influence on the V–O vibration frequency, which can be easily understood as the A ion is not directly involved in the vibrating bond.

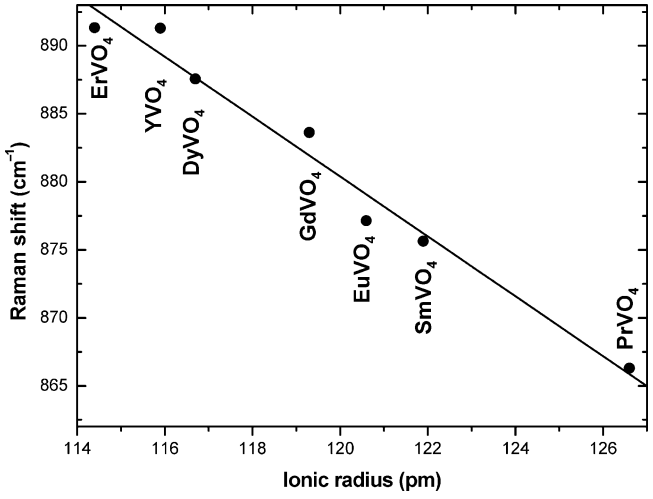

Figure 7. Evolution of Raman shift as a function of the A ionic radius in AVO_4 materials prepared by the molecular precursor route.

Additionally, scanning electron microscopy was used to characterise the morphology of the particles. As shown in Figure 8, YVO_4 prepared by conventional solid-state reaction exhibits quite large and irregular particles, while the same compound prepared from molecular precursors exhibits a totally different morphology, namely a slightly disordered porosity. This morphology was already observed for Nb-Ta oxides prepared by the same soft chemistry route.[16] Nevertheless, some AVO_4 materials display another kind of morphology, as $PrVO_4$ which seems to present a higher crystallinity with elongated and spherical particles.

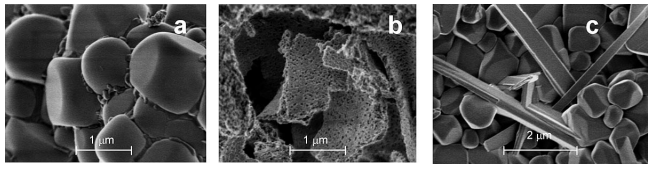

Figure 8. SEM images of pure (a) YVO_4 oxide prepared by the ceramic method, (b) YVO_4 oxide and (c) $GdVO_4$ prepared by the molecular precursor method.

$Y_{1-x}Ln_xVO_4$ (Ln = Gd, Pr)

Because yttrium vanadate and lanthanide vanadates present the same crystallographic structure, the preparation of $Y_{1-x}Ln_xVO_4$ (Ln = Gd, Pr) with x = 0, 0.1, 0.3, 0.5, 0.7, 0.9 and 1 was performed in order to obtain solid solutions between YVO_4 and $LnVO_4$. For this purpose, XRD was implemented and the lattice parameters as well as the lattice volume were calculated according to the zircon-type tetragonal structure. Figure 9 displays the evolution of the lattice volume as a function of the composition x for $Y_{1-x}Pr_xVO_4$ and $Y_{1-x}Gd_xVO_4$. The results put forward a linear increase of the lattice parameter when the Ln^{III} content increases. This behaviour follows the Vegard's law, and it is indicative of the presence of a solid solution in the whole composition range.

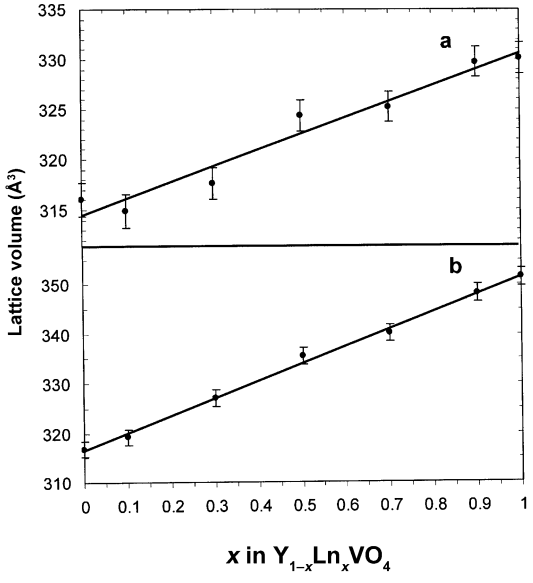

Figure 9. Evolution of the lattice volume as a function of x in (a) $Y_{1-x}Gd_xVO_4$ and (b) $Y_{1-x}Pr_xVO_4$.

Raman spectra of the samples were also recorded, and the V–O bond Raman shift was monitored and plotted as a function of the composition x (Figure 10). As for XRD analyses, a linear correlation between the Raman shift and the Ln^{III} content is observed in both cases. This confirms the presence of the solid solution already evidenced by XRD.

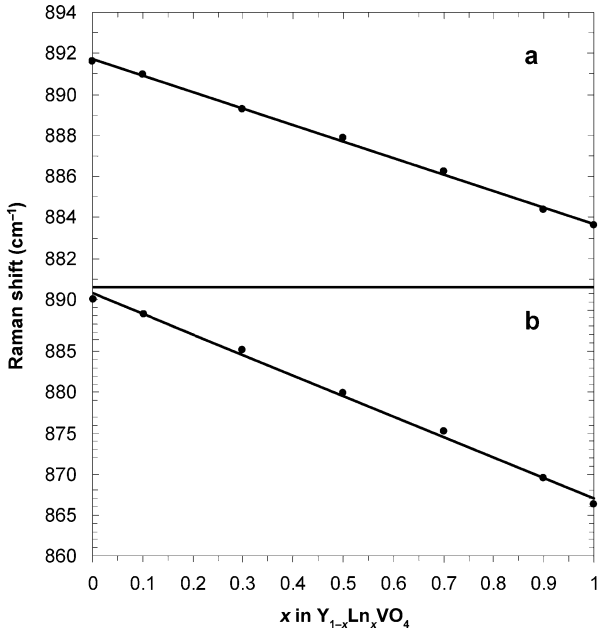

Figure 10. Evolution of the Raman shift of the V–O vibration as a function of x in (a) $Y_{1-x}Gd_xVO_4$ and (b) $Y_{1-x}Pr_xVO_4$.

Conclusions

Zircon-type yttrium and lanthanide vanadates have been successfully prepared by a soft chemistry route using coordination compounds as molecular precursors at a moderate temperature of 800 °C. The synthesis of single zircon-type phases was confirmed by X-ray diffraction for all the AVO_4 compounds. It appears that the substitution of a lanthanide ion for another one leads to a modification of the lattice parameters but does not modify the structure of the mixed oxides. Furthermore, a linear correlation between lattice parameters and the Ln ionic radius was observed. The Raman spectra confirmed the XRD analyses and a linear correlation between the Raman shift of the V–O vibration and the ionic radius was also observed. Solid solutions $Y_{1-x}Pr_xVO_4$ and $Y_{1-x}Gd_xVO_4$ were successfully prepared by the same pathway as evidenced by XRD and Raman analyses.

Experimental Section

Materials/Solvents: All products were analytical reagent grade and were used without further purification. Ethylenediaminetetraacetic acid, H_4EDTA, was purchased from Fluka. Ammonium metavanadate, NH_4VO_3, was supplied from Acros. Yttrium nitrate, $Y(NO_3)_3\cdot 6H_2O$, was purchased from Aldrich. Erbium carbonate, $Er_2(CO_3)_3\cdot 2.1H_2O$, europium oxide, Eu_2O_3, gadolinium carbonate, $Gd_2(CO_3)_3\cdot H_2O$, praseodymium carbonate, $Pr_2(CO_3)_3\cdot 8H_2O$, samarium oxide, Sm_2O_3, and dysprosium carbonate, $Dy_2(CO_3)_3\cdot 4H_2O$, were supplied from Alfa Aesar. For erbium and gadolinium carbonate, the total water amount was determined by thermogravimetric analysis and elemental analysis. Aqueous ammonia (35 wt.-%), ethanol and diethyl ether were used as received.

Methods: Elemental analysis was carried out at the University College, London, UK. Thermogravimetric analyses were carried out under flowing air (100 mL min^{-1}) with a Mettler Toledo 851e thermogravimetric analyser applying a heating rate of 10 °C min^{-1}. Differential thermal analyses were performed simultaneously on the same apparatus. Powder X-ray diffraction data were collected with a Siemens D5000 diffractometer using the Cu-K_α line (λ = 0.15418 nm). X-ray thermodiffractometry was performed with the same apparatus. In this case, the XRD patterns were recorded at room temperature and then between 500 and 800 °C, after waiting for 2 h at each temperature selected. The temperature was finally decreased again to room temperature, and an XRD pattern was recorded. FT-Raman spectra were taken with a Bruker RFS100/S spectrometer at a wavelength of 1064 nm. Scanning electron microscopy (SEM) was performed with a Gemini Digital Scanning Microscope 982 with 1 kV accelerating voltage. Nano-electrospray ionisation mass spectrometry (nESI-MS) measurements were obtained with a Thermo Finnigan TSQ Quantum instrument. The samples were introduced by injection of a 0.001 mol L^{-1} solution of the complex dissolved in CH_3OH/H_2O (1:1, v/v).

Preparation of the Coordination Complexes

$(NH_4)_3[V(O)_2(EDTA)]\cdot 0.5H_2O$: The synthesis pathway of this compound was adapted from a procedure used by Lee et al. to obtain the PDTA derivative[25] and was published in a previous paper.[16] Yield: 80%. $C_{10}H_{25}N_5O_{10.5}V$ (434.27): calcd. C 27.65, H 5.80, N 16.13; found C 28.13, H 5.82, N 16.22. MS (nESI): m/z = 373.01 $[H_2ML]^-$.

$(NH_4)[Y(EDTA)]\cdot 3H_2O$: A slurry of H_4EDTA (2 g, 6.84 mmol) in distilled water (200 mL) was heated under reflux to obtain a homogeneous solution. Yttrium nitrate (2.62 g, 6.84 mmol) was then gradually added. When the solid was totally dissolved, ammonia (6 M) was added dropwise to reach a pH value between 7 and 8. The mixture was then heated under reflux for 24 h. After solvent evaporation under reduced pressure to a final volume of 10 mL, the addition of ethanol (35 mL) yielded a white solid which was filtered off, washed with ethanol and diethyl ether and air-dried. Yield: 2.62 g (79%). $C_{10}H_{22}N_3O_{11}Y$ (449.20): calcd. C 26.74, H 4.93, N 9.35; found C 26.54, H 4.55, N 8.70. MS (nESI): m/z = 376.63 $[ML]^-$.

$(NH_4)[Pr(EDTA)]\cdot 7H_2O$: This Pr compound was prepared according to the same procedure as used for the yttrium complex but replacing yttrium nitrate by praseodymium carbonate. The complex was isolated as a light-green powder. Yield: 1.46 g (37%). $C_{10}H_{30}N_3PrO_{15}$ (573.26): calcd. C 20.95, H 5.27, N 7.33; found C 21.32, H 4.77, N 7.30. MS (nESI): m/z = 428.74 $[ML]^-$.

$(NH_4)[Sm(EDTA)]\cdot 8H_2O$: This Sm compound was prepared according to the same procedure as used for the yttrium complex but replacing yttrium nitrate by samarium oxide. The complex was isolated as a white powder. Yield: 3.24 g (79%). $C_{10}H_{32}N_3O_{16}Sm$ (600.67): calcd. C 19.99, H 5.37, N 6.99; found C 20.69, H 4.64, N 6.94. MS (nESI): m/z = 439.60 $[ML]^-$.

$(NH_4)[Eu(EDTA)]\cdot 7.5H_2O$: This Eu compound was prepared according to the same procedure as used for the yttrium complex but replacing yttrium nitrate by europium oxide. The complex was isolated as a white powder. Yield: 3.57 g (88%). $C_{10}H_{31}EuN_3O_{15.5}$ (593.32): calcd. C 20.24, H 5.27, N 7.08; found C 20.40, H 5.15, N 7.04. MS (nESI): m/z = 440.62 $[ML]^-$.

$(NH_4)[Gd(EDTA)]\cdot 7H_2O$: This Gd compound was prepared according to the same procedure as used for the yttrium complex but replacing yttrium nitrate by gadolinium carbonate. The complex was isolated as a white powder. Yield: 3.02 g (75%). $C_{10}H_{30}GdN_3O_{15}$ (589.61): calcd. C 20.37, H 5.13, N 7.13; found C 20.35, H 4.94, N 6.94. MS (nESI): m/z = 445.20 $[ML]^-$.

$(NH_4)[Dy(EDTA)]\cdot 6H_2O$: This Dy compound was prepared according to the same procedure as used for the yttrium complex but replacing yttrium nitrate by dysprosium carbonate. The complex was isolated as a white powder. Yield: 2.29 g (58%). $C_{10}H_{28}DyN_3O_{14}$ (576.84): calcd. C 20.82, H 4.89, N 7.28; found C 20.94, H 4.75, N 6.43. MS (nESI): m/z = 449.93 $[ML]^-$.

$(NH_4)[Er(EDTA)]\cdot 2H_2O$: This Er compound was prepared according to the same procedure as used for the yttrium complex but replacing yttrium nitrate by erbium carbonate. The complex was isolated as a light-pink powder. Yield: 2.44 g (70%). $C_{10}H_{20}ErN_3O_{10}$ (509.54): calcd. C 23.57, H 3.96, N 8.25; found C 23.25, H 3.64, N 8.05. MS (nESI): m/z = 455.58 $[ML]^-$.

AVO_4 Compounds Prepared by the Molecular Precursor Method: Figure 11 describes the preparation Scheme for mixed A-V-O compounds (A = Y and/or Ln). The corresponding coordination compounds were dissolved separately in distilled water and then mixed together in appropriate proportions. The resulting clear solution was then stirred at room temperature for 1 h and, after removal of the solvent under reduced pressure, a mixed solid precursor was obtained. This solid precursor was precalcined in air at 300 °C for 2 h and then calcined in air at 800 °C for 6 h to yield the mixed oxide.

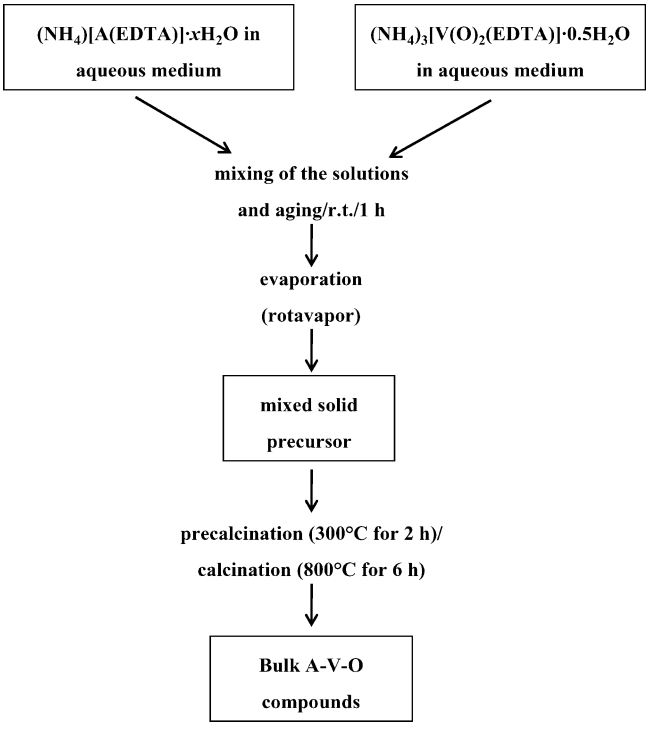

Figure 11. Process chart for the A-V-O preparation according to the molecular precursor method.

YVO_4 Oxide Prepared by the Ceramic Method: YVO_4 was also prepared by a conventional solid-state reaction between yttrium carbonate (0.95 g, 2.45 mmol) and ammonium metavanadate (0.57 g, 4.91 mmol) described in the literature.[13] These solid starting materials were ground in an agate mortar and calcined in air at 800 °C for 10 h. The resulting powder was ground again and calcined in air at 1000 °C for 10 h.

Acknowledgments

The authors thank the Belgian National Fund for Scientific Research (FNRS) for financial support. This work was also supported by a fellowship allotted to N. D. by the "Fonds pour la Recherche dans l'Industrie et l'Agriculture" (F.R.I.A.), Belgium. This work has been performed in the frame of the Interuniversity Attraction Poles Programme of the Belgian State, Belgian Science Policy, Project INANOMAT, P6/17.

[1] a) Z. M. Fang, Q. Hong, Z. H. Zhou, S. J. Dai, W. Z. Weng, H. L. Wan, *Catal. Lett.* **1999**, *61*, 39–44; b) C. T. Au, W. D. Zhang, H. L. Wan, *Catal. Lett.* **1996**, *37*, 241–246.
[2] a) H. Wang, Y. Q. Meng, H. Yan, *Inorg. Chem. Commun.* **2004**, *7*, 553–555; b) U. O. Krasovec, B. Orel, R. Reisfeld, *Electrochem. Solid-State Lett.* **1998**, *1*, 104–106.
[3] G. J. Bowden, *Aust. J. Phys.* **1998**, *51*, 201–236.
[4] A. H. Cooke, C. J. Ellis, K. A. Gehring, M. J. M. Leask, D. M. Martin, B. M. Wanklyn, M. R. Wells, R. L. White, *Solid State Commun.* **1970**, *8*, 689–692.
[5] A. K. Levine, F. C. Palilla, *Appl. Phys. Lett.* **1964**, *5*, 118–120.
[6] G. Blasse, B. C. Grabmaier, *Luminescent Materials*, Springer-Verlag, Berlin, **1994**.
[7] T. Jensen, V. G. Ostroumov, J. P. Meyn, G. Huber, A. I. Zagumennyi, I. A. Shcherbakov, *Appl. Phys. B: Lasers Opt.* **1994**, *58*, 373–379.
[8] a) K. Gaur, A. K. Tripathi, H. B. Lal, *J. Mater. Sci. Lett.* **1983**, *2*, 371–374; b) K. Gaur, H. B. Lal, *J. Mater. Sci. Lett.* **1983**, *2*, 744–746.
[9] A. Huignard, T. Gacoin, J. P. Boilot, *Chem. Mater.* **2000**, *12*, 1090–1094.
[10] a) H. Wu, H. F. Xu, Q. Su, T. H. Chen, M. M. Wu, *J. Mater. Chem.* **2003**, *13*, 1223–1228; b) G. H. Pan, H. W. Song, X. Bai, Z. X. Liu, H. Q. Yu, W. H. Di, S. W. Li, L. B. Fan, X. G. Ren, S. Z. Lu, *Chem. Mater.* **2006**, *18*, 4526–4532.
[11] W. D. Zhang, C. T. Au, H. L. Wan, *Appl. Catal. A* **1999**, *181*, 63–69.
[12] B. C. Chakoumakos, M. M. Abraham, L. A. Boatner, *J. Solid State Chem.* **1994**, *109*, 197–202.
[13] H. W. Zhang, X. Y. Fu, S. Y. Niu, G. Q. Sun, Q. Xin, *J. Solid State Chem.* **2004**, *177*, 2649–2654.
[14] a) X. Q. Su, B. Yan, *Mater. Chem. Phys.* **2005**, *93*, 552–556; b) X. Z. Xiao, B. Yan, *J. Non-Cryst. Solids* **2006**, *352*, 3047–3051.
[15] H. Wullens, D. Leroy, M. Devillers, *Int. J. Inorg. Mater.* **2001**, *3*, 309–321.
[16] D. A. Bayot, M. M. Devillers, *Chem. Mater.* **2004**, *16*, 5401–5407.
[17] D. A. Bayot, M. M. Devillers, *Inorg. Chem.* **2006**, *45*, 4407–4412.
[18] H. Wullens, N. Bodart, M. Devillers, *J. Solid State Chem.* **2002**, *167*, 494–507.
[19] a) L. K. Templeton, D. H. Templeton, A. Zalkin, H. W. Ruben, *Acta Crystallogr., Sect. B* **1982**, *38*, 2155–2159; b) J. Wang, Z. R. Liu, X. D. Zhang, W. G. Jia, H. F. Li, *J. Mol. Struct.* **2003**, *644*, 29–36; c) N. Sakagami, Y. Yamada, T. Konno, K. Okamoto, *Inorg. Chim. Acta* **1999**, *288*, 7–16; d) J. Wang, X. D. Zhang, Y. Zhang, Z. R. Liu, *Wuhan Univ. J. Nat. Sci.* **2003**, *8*, 1131–1137.
[20] X. Wang, I. Loa, K. Syassen, M. Hanfland, B. Ferrand, *Phys. Rev. B* **2004**, *70*, 064109/1–064109/6.
[21] R. D. Shannon, *Acta Crystallogr., Sect. A* **1976**, *32*, 751–767.
[22] A. Jayaraman, G. A. Kourouklis, G. P. Espinosa, A. S. Cooper, L. G. Vanuitert, *J. Phys. Chem. Solids* **1987**, *48*, 755–759.
[23] S. J. Duclos, A. Jayaraman, G. P. Espinosa, A. S. Cooper, R. G. Maines, *J. Phys. Chem. Solids* **1989**, *50*, 769–775.
[24] M. E. Escobar, E. J. Baran, *Z. Naturforsch., Teil A* **1980**, *35*, 1110–1111.
[25] M.-H. Lee, *Anal. Sci.* **2001**, *17*, a235–a238.

Received: September 12, 2007
Published Online: November 15, 2007

